



# Removal of Reactive Dyes from Aqueous Solution by Fenton Reaction: Kinetic Study and Phytotoxicity Tests

Marcela G. R. Tavares · Danilo H. S. Santos · Mariana G. Tavares · José L. S. Duarte  · Lucas Meili · Wagner R. O. Pimentel · Josealdo Tonholo · Carmem L. P. S. Zanta

Received: 8 December 2019 / Accepted: 5 February 2020 / Published online: 13 February 2020  
© Springer Nature Switzerland AG 2020

**Abstract** Fenton process was successfully applied to degrade three reactive dyes, blue 19 (RB19), red 195 (RR195), and yellow 145 (RY145), a mixture of dyes and a real textile effluent. A  $2^3$  full factorial design coupled with a response surface methodology (RSM) was conducted to evaluate the effects of  $H_2O_2$ ,  $Fe^{2+}$ , and dye concentration on the Fenton reaction measured by absorbance reduction (AR) as response. Considering the analysis of variance (ANOVA), the statistical models could be used to describe experimental results and to predict the process behavior. The results obtained by RSM indicated that the optimum conditions for Fenton were  $[H_2O_2] = 50 \text{ mg L}^{-1}$ ,  $[Fe^{2+}] = 0.5 \text{ mmol L}^{-1}$ , and dye concentration =  $0.075 \text{ g L}^{-1}$ , obtaining up to 90% of AR. From kinetic study, the absorbance reduction for RY145 followed a second-order model, while RB19 and RR195 followed a first-order model. The mixture of

dyes and the real textile effluent obtained lower AR, 56% and 22%, respectively. The phytotoxicity tests indicate that the Fenton reactions were very effective to reduce the toxicity of almost all contaminated solutions; however, for more complex solution (mixture of dyes and real effluents), a longer reactional time is necessary. Therefore, the results pointed that the Fenton reaction is very efficient in solution discoloration.

**Keywords** Fenton · Mixture of dyes · Textile effluents, real effluent · Toxicity

## 1 Introduction

Among all industrial segments, the wastewater generated in textile industry was considered the most polluting and toxic. Dyes are widely used in textile industries and their presence in effluents can cause harmful effects on aquatic environments in terms of chemical and biological oxygen demand. Besides that, these compounds are carcinogenic, mutagenic, and allergic for humans and animals, even at low concentrations. Dyes usually have a complex aromatic molecular structure giving them stable characteristics which provide a great difficulty to biodegradation. Moreover, dye-contaminated effluents have large loads of suspended solids, fluctuating pH, and heat and light stability (Shuang et al. 2008; Aksakal and Uzun 2010; Kalkan et al. 2012; Kadam et al. 2013; Mahmoud et al. 2016; Elmoubarki et al. 2017; Priya et al. 2019; dos Santos et al. 2019a).

M. G. R. Tavares · D. H. S. Santos · M. G. Tavares · J. L. S. Duarte · J. Tonholo · C. L. P. S. Zanta  
Laboratory of Applied Electrochemistry, Institute of Chemistry and Biotechnology, Federal University of Alagoas, Campus A.C. Simões, Maceió, AL CEP 57072-970, Brazil

J. L. S. Duarte (✉) · L. Meili  
Laboratory of Processes (LaPro), Center of Technology, Federal University of Alagoas, Campus A. C. Simões, Lourival Melo Mota Av., Br 101 Norte, Km 97, Tabuleiro dos Martins, Maceió, AL, Brazil  
e-mail: leandrosduarte@yahoo.com.br

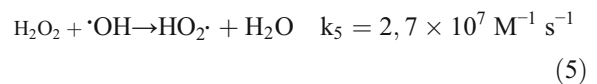
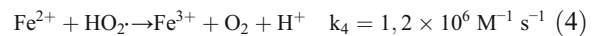
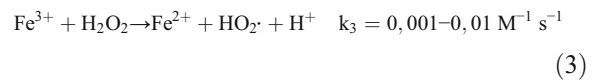
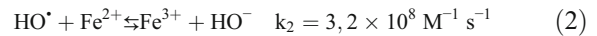
W. R. O. Pimentel  
Center of Technology, Federal University of Alagoas, Campus A. C. Simões, Lourival Melo Mota Av., Br 101 Norte, Km 97, Tabuleiro dos Martins, Maceió, AL, Brazil

Reactive dyes (RD) are the second most used dye kind in textile industries for dyeing cellulose fibers due to its characteristics of bright color, water solubility, and ease application. RD have several features that hamper its removal from effluents by conventional separation processes as high solubility in water, cannot be reused once they become non-reactive due to hydrolysis, low adsorption, and fixation in the fibers generating dye effluent with high concentration. Thus, dye effluent contaminated with RD is the most difficult to treat by conventional processes (Asgher 2012; Khatri et al. 2015; Hassan and Carr 2018).

In the last decades, several physical, chemical, and biological techniques have been studied to remove dyes from water and wastewater such as adsorption (Weber et al. 2013; Meili et al. 2017; Nascimento et al. 2018; Georgin et al. 2019; Meili et al. 2019a, b; dos Santos et al. 2019b), coagulation/flocculation (Zafar et al. 2018; Qiu et al. 2018; Guo et al. 2019; Bahrpaima and Fatehi 2019; Luo et al. 2019; Song et al. 2019; Dotto et al. 2019), filtration (Hatimi et al. 2018; Zhijiang et al. 2018; Liu et al. 2018; Zhou et al. 2019), and advanced oxidative processes (AOPs) as electrochemical processes (Duarte et al. 2013; Mook et al. 2017; Duarte et al. 2018; Sathishkumar et al. 2019; Gui et al. 2019; Li et al. 2019; Vasconcelos et al. 2016; Duarte et al. 2019), Fenton and modified Fenton reactions (Panizza and Oturan 2011; Thiam et al. 2015; Sohrabi et al. 2017; Çiner 2018; Gonçalves et al. 2019; Azha et al. 2019), and others.

Advanced oxidative processes (AOPs) are very promising techniques to remove a wide range of organic compounds. Among which, Fenton reaction is an attractive alternative process due to its high effectiveness at room temperature, easy operation, reagent availability, rapid reactions, and short treatment times (Boczkaj and Fernandes 2017; Rosales et al. 2018; Gagol et al. 2018; Silva De Lima et al. 2019; Wang et al. 2019). Fenton process is based on the use of  $\text{H}_2\text{O}_2$  in the presence of ferrous ions ( $\text{Fe}^{2+}$ ) to generate a highly oxidant species as hydroxyl radicals ( $\cdot\text{OH}$ ) (Miklos et al. 2018). Hydroxyl radicals have high standard potential ( $E^0 = 2.80 \text{ V}$ ) allowing the degradation of almost all organic chemicals. This reaction causes a non-selective mineralization of organic compounds to  $\text{CO}_2$ ,  $\text{H}_2\text{O}$ , and inorganic ions (Silva De Lima et al. 2019). Fenton reaction comprises a simple redox reaction in which  $\text{Fe}^{2+}$  ions are oxidized to  $\text{Fe}^{3+}$ , and  $\text{H}_2\text{O}_2$  is reduced to hydroxyl ion and a hydroxyl radical, whose steps are presented in

reactions 1–5 (Nogueira et al. 2007; dos Santos et al. 2019a).



In a Fenton classical laboratory experiment, the optimization is executed varying one of the independent parameters while maintaining the other variables fixed. This procedure requires many experimental runs, consuming time and financial resources. A strategy to work around this problem is the use of a response surface methodology (RSM). RSM is a multivariate statistical and mathematical technique which helps to evaluate the relationship between the variables used for modeling and optimizing processes. This method permits to reduce the number of experiments and to determine the optimum operational condition (Shamsuddin et al. 2015; Liu et al. 2017; Kaynar et al. 2018; Amiri et al. 2019).

Effluents are complex mixtures of diverse substances and AOPs may produce toxic by-products during the reactions. Then, the toxicity of effluent after treatment would enhance or reduce. Therefore, several organisms are used to evaluate the biological effects caused by toxicants. These toxicity tests may be performed using vascular plant species to assess the adverse effects on seed germination and seedling development during the initial growth (Wang and Freemark 1995; Tchounwou et al. 2001; Young et al. 2012). Lettuce seeds (*Lactuca sativa*) are excellent option for toxicity bioassays, once they are highly sensitive to chemical stress and germinate fast. The phytotoxicity procedure consists in the measure of root growth and the germination rate (Tavares et al. 2016).

Considering the importance of reactive dyes in textile industry and their recalcitrant characteristics, this work aims to evaluate the efficiency of the Fenton reaction in the removal of three different RD (reactive blue 19, reactive red 195, and reactive yellow 145). A  $2^3$  full factorial design of experiments coupled with a response surface methodology (RSM) was conducted to evaluate the effects of  $H_2O_2$ , ions  $Fe^{+2}$ , and dye concentration on the Fenton reaction considering the absorbance reduction (AR) as response. With the previously optimized operational conditions (Tavares et al. 2016), the kinetic of Fenton reaction was studied. Phytotoxicity tests were performed to evaluate the ecotoxicity of treated solutions. Finally, to assess the efficiency of studied process, tests with mixture of dyes and with a real effluent were conducted.

## 2 Materials and Methods

### 2.1 Chemicals

Commercial Reactive Blue 19 (RB19), Reactive Red 195 (RR19), and Reactive Yellow 145 (RY145) were purchased from Araquímica (Brazil) and used as received. Chemicals for Fenton reaction, hydrogen peroxide ( $H_2O_2$ ), and ferrous sulfate ( $FeSO_4 \cdot 7H_2O$ ) were obtained from VETEC (Brazil). Table 1 shows the chemical structures of the dyes.

### 2.2 Fenton Experiments and Experimental Design

Fenton reactions were conducted in an agitated batch reactor using 100 mL of dye solution with pH adjusted to  $3.0 \pm 0.1$  for 1 h. pH was adjusted using sulfuric acid ( $0.1 \text{ mol L}^{-1}$ ) and sodium hydroxide ( $0.1 \text{ mol L}^{-1}$ ). The coloring reduction was monitored by UV-Vis spectrometry (Shimadzu/Multispec-1501). Absorbance was measured in the wavelength of greater absorbance (RY145 = 422 nm, RR195 = 542 nm, and RB19 = 591 nm), and for the mixture, the coloring reduction was determined by the integration of the spectral area.

A  $2^3$  full factorial experiment design coupled with a response surface methodology (RSM) was conducted to evaluate the effects of independent parameters on dependent variable (response). Independent factors considered in this work were the Fenton reactants,  $H_2O_2$  ( $X_1$ ) and ion  $Fe^{2+}$  ( $X_2$ ) concentration in  $\text{mmol L}^{-1}$ , and dye concentration ( $X_3$ ) RY145, RR195, and RB19 in

$\text{g L}^{-1}$ , whereas absorbance reduction (%) - Y was the response variable (dependent variable). The total number of experiments were given by  $2^k$  ( $2^k$ , factorial runs; k, the number of independent process variables), giving eight experiments performed in duplicate. The high and low levels of each independent variable and the matrix of design with the respective absorbance reduction are presented in Tables 2 and 3, respectively.

The Eq. 6 was used to predict the optimum condition of dye removal. Analysis of variance (ANOVA) was used to validate the adequacy of model.

$$Y = b_0 + \sum_{i=1}^n b_i x_i + \sum_{i=1}^n b_{ii} x_i^2 + \sum_{i=1}^{n-1} \sum_{j=2}^n b_{ij} x_i x_j + \epsilon \quad (6)$$

where Y is the response;  $b_0$  represents the intercept;  $b_{ij}$ ,  $b_{ii}$ , and  $b_i$  are the coefficients; n, number of variables;  $x_i$  and  $x_j$ , independent variables; and  $\epsilon$ , the error (Kaynar et al. 2018; Xia et al. 2018).

### 2.3 Phytotoxicity Tests

Bioassays were performed using lettuce (*Lactuca sativa*) germination method based on Young et al. (2012). Ten seeds were placed in Petri dishes on filter papers soaked with 5 mL of treated solution. Chronic toxicity tests were conducted, in triplicate, for several effluents' concentration (12.5%, 25%, 50%, and 100%) and negative control was performed with distilled water. Plates were taken to incubator at  $22 \text{ }^\circ\text{C} \pm 2 \text{ }^\circ\text{C}$  for 120 h (5 days). The numbers of germinated seeds and the radicle length were determined. With these data, it was possible to calculate the relative length (RL), relative germination (RG), and the germination index (GI) through Eqs. 7, 8, and 9.

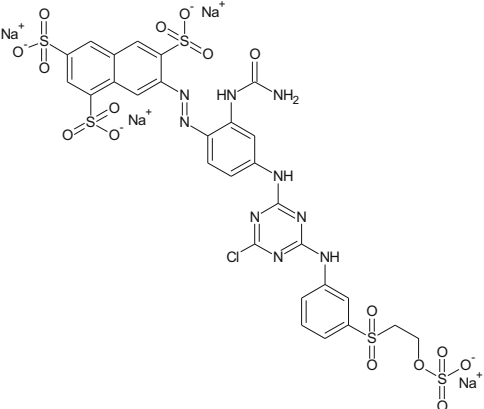
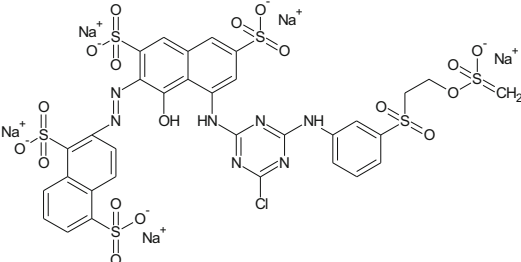
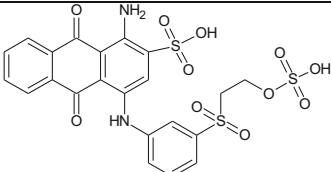
$$RL = \frac{RLS}{RLC} * 100 \quad (7)$$

$$RG = \frac{GSS}{GSC} * 100 \quad (8)$$

$$GI = \frac{RL * RG}{100} \quad (9)$$

where RLS is the root length of the sample, RLC is the radius length of the control, GSS is the germinated seeds of the sample, and GSC is the germinated seeds of the control.

**Table 1** Characteristics of dyes

Dye	Molecular Form	Chemical Structure	Molecular Weight (g.mol <sup>-1</sup> )
Reactive Yellow 145	C <sub>28</sub> H <sub>20</sub> ClN <sub>9</sub> Na <sub>4</sub> O <sub>16</sub> S <sub>5</sub>		1,026.26
Reactive Red 195	C <sub>31</sub> H <sub>19</sub> ClN <sub>7</sub> Na <sub>5</sub> O <sub>19</sub> S <sub>6</sub>		1,136.32
Reactive Blue 19	C <sub>22</sub> H <sub>18</sub> N <sub>2</sub> O <sub>11</sub> S <sub>3</sub>		582.6

### 3 Results and Discussion

#### 3.1 Experimental Design and RSM

The 2<sup>3</sup> full factorial design of experiments was used to establish the best conditions of H<sub>2</sub>O<sub>2</sub>, ion Fe<sup>2+</sup>, and dye

**Table 2** Factors and levels used in DOE

Variables	Levels	
	(-)	(+)
X <sub>1</sub> -concentration of H <sub>2</sub> O <sub>2</sub> (mg L <sup>-1</sup> )-C <sub>peroxide</sub>	10	50
X <sub>2</sub> -Concentration of ion Fe <sup>2+</sup> (mmol.L <sup>-1</sup> )-C <sub>Fe</sub>	0.1	0.5
X <sub>3</sub> -concentration of dye (g L <sup>-1</sup> )-C <sub>dye</sub>	0.075	0.75

concentration seeking to maximize the absorbance reduction (%). From the Pareto's chart presented in Fig. 1, it is possible to determine the statistically significant variables for each design regarding RY145, RB19, and RR195 considering 95% of confidence interval.

For RY145 (Fig. 1a), all independent variables and their interactions were significant. Lower level of X<sub>3</sub> and the interaction X<sub>1</sub>X<sub>3</sub> has shown greater effect in the process. Higher absorbance reduction values were obtained for the runs using the lower dye concentration (tests 1 to 4) and when X<sub>1</sub> and X<sub>3</sub> are combined in the same levels (tests 1 and 8). Initial pollutant concentration is an important parameter in Fenton reactions affecting the degradation effectiveness. The excessive presence of organic compounds can act as a barrier to the reaction between <sup>•</sup>OH and ferrous ions Fe<sup>2+</sup> (Bulut

**Table 3** Matrix of design and absorbance reduction

Test	$X_1$ -C <sub>peroxide</sub> (mmol L <sup>-1</sup> )	$X_2$ -C <sub>Fe</sub> (mmol L <sup>-1</sup> )	$X_3$ -C <sub>dye</sub> (g L <sup>-1</sup> )	Y. Absorbance reduction (%)		
				RY145	RB19	RR195
1	10	0.1	0.075	95.70	99.70	99.50
2	50	0.1	0.075	88.10	99.20	98.30
3	10	0.5	0.075	92.10	98.50	98.40
4	50	0.5	0.075	86.00	96.40	97.90
5	10	0.1	0.75	80.20	39.60	80.20
6	50	0.1	0.75	88.60	54.90	87.10
7	10	0.5	0.75	81.30	55.60	88.80
8	50	0.5	0.75	98.40	91.30	99.60

and Aydin 2006).  $X_1$ , in the higher level, has a favorable effect in AR when combined with higher levels of  $X_3$ , since  $X_1X_3$  interaction had higher significance. Otherwise, the higher concentration of  $H_2O_2$  negatively affects the color removal. This behavior is related to the reaction between the excess of reactant with free hydroxyl radicals ( $\cdot OH$ ) producing hydroperoxyl ( $HO_2\cdot$ ), which is less reactive and does not contribute in the pollutant degradation. Besides, serial reactions may occur, consuming radicals that eventually reduce the general oxidative capacity (da Silva Duarte et al. 2019). The parameter  $X_2$ , although it was significant, had the lowest effect on AR. It is remarkable that at higher  $Fe^{2+}$  concentration, it obtained higher AR, which is more pronounced in higher levels of dye and hydrogen peroxide. Otherwise, this effect is not relevant in the lowest dye concentration level. In addition, negative effects of  $Fe^{2+}$  concentration on the response were observed. This behavior may be related to the increase in the substrate removal rate reaching a value that the increase of catalysts does not alter the reaction (Bulut and Aydin 2006).

For RB19, observing Fig. 1b, it is possible to note that parameter  $X_3$  showed the most pronounced effect, while  $X_2X_3$  and  $X_1X_3$  interaction presented virtually the same significance. The highest AR values were achieved in the tests using smaller dye concentration (tests 1 to 4) and those where the combination between  $X_1$  and  $X_3$ , as well  $X_2$  and  $X_3$ , occurs in the same levels (tests 1 and 8). Parameters  $X_1$  and  $X_2$  have greater effect on their higher levels; however, this behavior was only observed when  $X_3$  was at its upper level. It is not possible to observe the same using the lower dye concentration, since the greatest values of absorbance reduction were reached at smallest concentrations of

Fenton reactants ( $0.1 \text{ mmol L}^{-1} Fe^{2+}$  and  $10 \text{ mg L}^{-1} H_2O_2$ ).

For RR195, it was observed in Fig. 1c that  $X_3$  at the lowest level had more relevance, as well as interaction  $X_2X_3$ . Tests performed at lowest dye concentration (1 to 4) had high absorbance reduction regardless of the Fenton reactant concentration used, although they had greater effect of their higher levels. In the tests with the higher dye concentration, the variables  $X_1$  and  $X_2$  acted better at their higher levels.

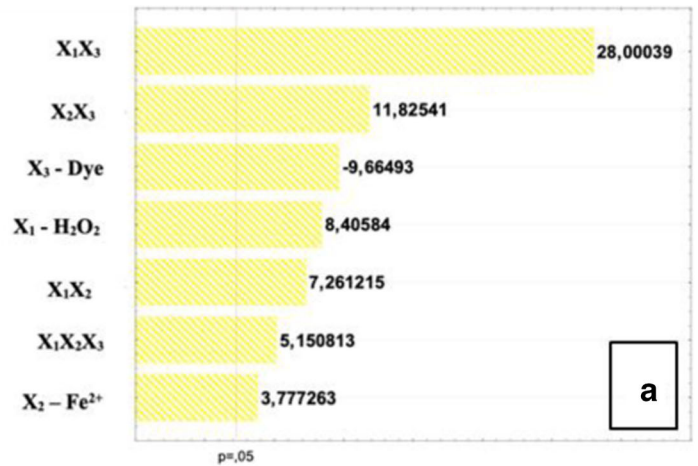
From the results presented, it was possible to obtain an equation that represents the response (absorbance reduction—Y) as function of independent variables,  $X_1$  (C<sub>peroxide</sub>),  $X_2$  (C<sub>Fe</sub>), and  $X_3$  (C<sub>dye</sub>). Therefore, statistical models of eight parameters related with each dye tested were obtained, RY145 (Eq. 10), RB19 (Eq. 11), and RR195 (Eq. 12).

$$\begin{aligned}
 Y = & 88.793 + 1.469X_1 \\
 & + 0.660X_2 - 1.689X_3 - 1.269X_1X_2 \\
 & + 4.893X_1X_3 + 2.066X_2X_3 \\
 & + 0.900X_1X_2X_3
 \end{aligned} \quad (10)$$

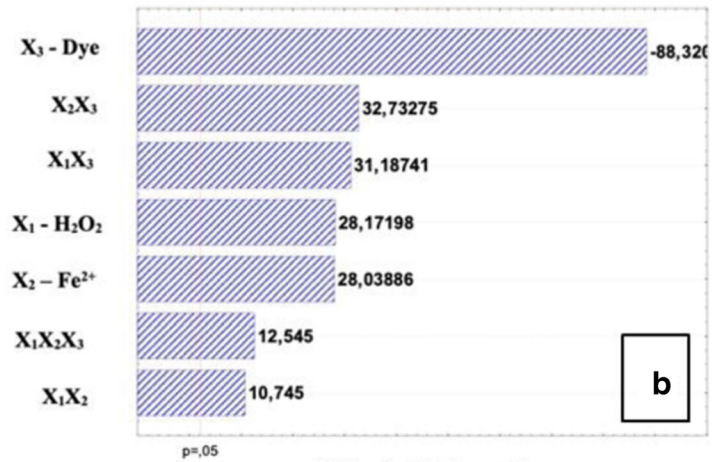
$$\begin{aligned}
 Y = & 79.374 + 6.059X_1 + 6.030X_2 - 19.050X_3 \\
 & + 2.345X_1X_2 + 6.710X_1X_3 + 7.044X_2X_3 \\
 & + 2.734X_1X_2X_3
 \end{aligned} \quad (11)$$



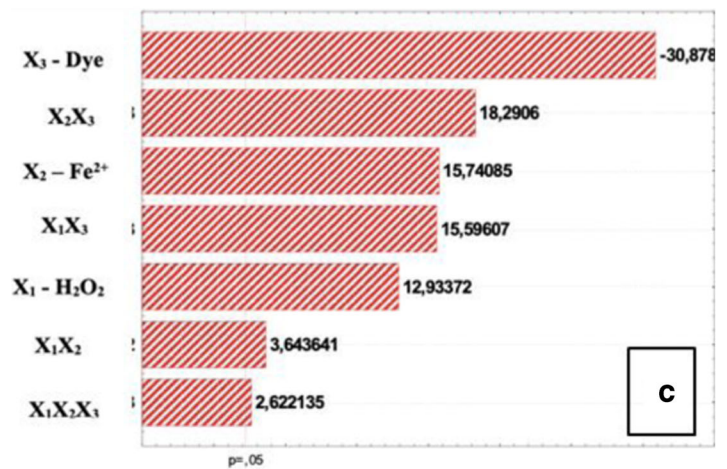
**Fig. 1** Pareto's chart: **a** RY145, **b** RB19, and **c** RR195



**Effects Estimation**



**Effects Estimation**



**Effects Estimation**

$$\begin{aligned}
 Y = & 93.726 + 2.006X_1 + 2.450X_2 - 4.802X_3 \\
 & + 0.562X_1X_2 + 2.427X_1X_3 + 2.839X_2X_3 \\
 & + 2.446X_1X_2X_3 \quad (12)
 \end{aligned}$$

To evaluate the statistical explanation of the above equations, the analysis of variance is given by Table 4. Statistical models are significant to describe experimental results and to predict the process behavior. The quality of adjustment was confirmed by the higher values of the coefficient of determination ( $R^2$ ).  $R^2$  values calculated for each dye, RR145, RB19 and RR195, indicate that 99.33%, 99.92%, and 99.24% of the total variation around the mean were explicated by the model, respectively.

In order to obtain the optimized conditions to treat the contaminated effluents using Fenton process, a RSM was performed; thus, three-dimensional surface graphs are presented in Fig. 2. Figure 2 a illustrates a response surface for RY145. Since interaction  $X_1X_3$  showed the highest significance, the surface was generated maintaining  $X_2$  fixed in its higher value. The highest AR were obtained when the dye was more concentrated. In its condition, Fenton reaction presented the best performance using the higher values of reactant concentration. Nevertheless, high response values were also achieved in lower Fenton reactant concentration.

Figure 2 b shows the response surface for RB16 to evaluate the interaction  $X_2X_3$ , since it was the most significant interaction, maintaining  $X_1$  fixed. The greatest absorbance reductions were achieved when the dye is more concentrated using the highest Fenton reactant concentration. However, the wide red zone observed shows that even in lower concentrations of peroxide and  $Fe^{2+}$  ions, it is possible to reach a satisfactory absorbance reduction.

Regarding the exposed results, it was possible to determine an optimized operational condition for the three dyes degradation:  $X_1$  ( $C_{\text{peroxide}}$ ) = 50 mg  $L^{-1}$ ;  $X_2$  ( $C_{Fe}$ ) = 0.5 mmol  $L^{-1}$ , and  $X_3$  ( $C_{\text{dye}}$ ) = 0.075 g  $L^{-1}$ .

### 3.2 Degradation Kinetic Study

Figure 3 presents the absorbance reduction as function of time for the three dyes at 0.075 g  $L^{-1}$  and 0.75 g  $L^{-1}$ . All dyes showed that high reductions were observed mainly using the biggest concentrations of  $Fe^{2+}$ , presenting almost complete removal in first minutes. In all

**Table 4** ANOVA

Dye	SV	QS	DF	QM
RY145	Regression	577.13	7	96.19
	Waste	3.91	8	0.43
	Total	581.03	15	
	% Explained variation	99.33		
RB19	SV	QS	DF	QM
	Regression	8697.60	7	1242.50
	Waste	6.87	8	0.86
	Total	8704.47	15	
	% Explained variation	99.92		
RR195	SV	QS	DF	QM
	Regression	757.75	7	126.29
	Waste	5.83	8	0.65
	Total	763.58	15	
	% Explained variation	99.24		

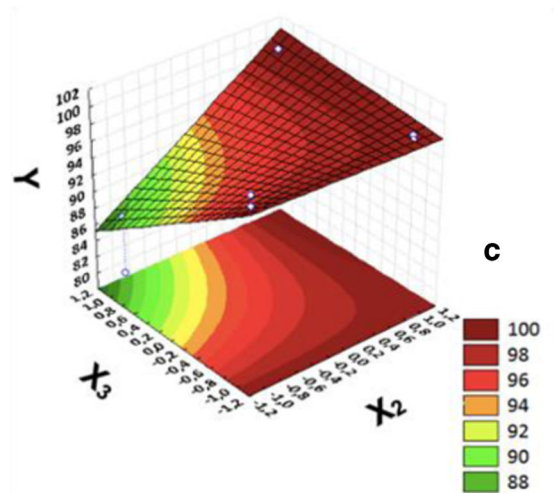
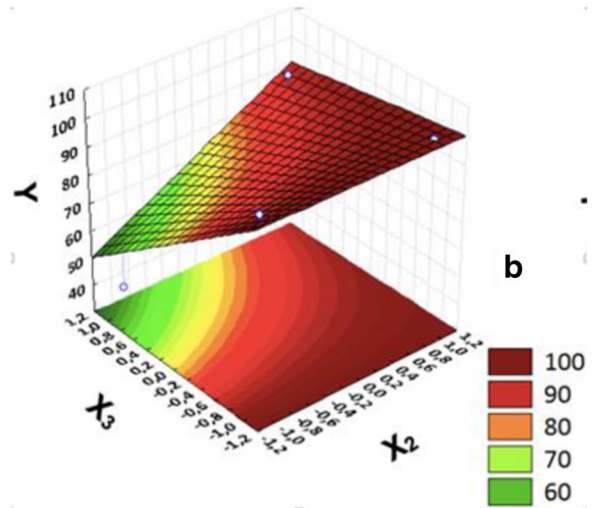
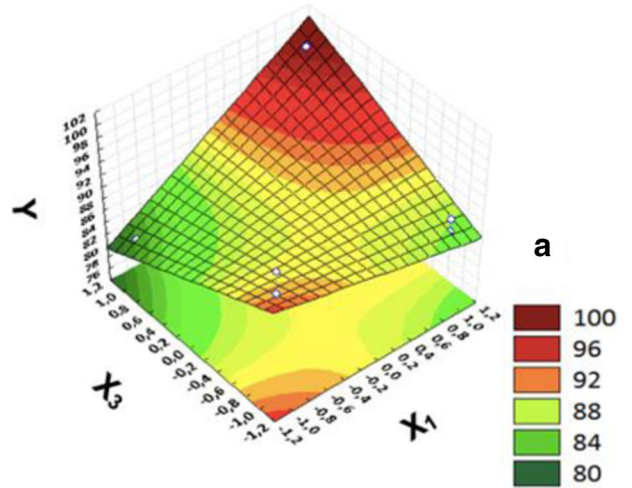
conditions, AR around 100% was observed. The exception was RY145 (Fig. 3a), where tests 2 and 4 differ from the others, reaching reduction values of 86 and 88%, respectively. Moreover, at higher pollutant concentration, it is perceived that the increase in Fenton reaction effectiveness is directly related to the increase in Fenton reactant concentration. RY145 and RR195 (Fig. 3d and e, respectively) presented a similar behavior, with degradations above 80% for all tests. However, for RB19 (Fig. 3f), the AR was more gradual. Only in the test 8, using higher peroxide and iron concentrations, significant reductions were obtained.

Kinetic constants were determined for each test based on the best fit of the kinetic model to experimental data. Kinetics study evaluates the speed of chemical reactions based on the change in reactant or product concentration in the time interval in which the reaction occurs. In a first-order reaction, the rate is proportional to the first power of the reagent concentration; if the concentration is doubled, the rate will also double. For a second-order reaction in which the A and B initial reactant concentrations are equal, the rate is proportional to the second power of the reagent concentration. If the concentration of the reagents is doubled, the speed is quadrupled (Atkins and Paula 2009).

The simplified mechanism of dye degradation can be represented by reactions 13 and 14 (Sun et al. 2007):



**Fig. 2** Response surfaces: **a** RY145, **b** RB19, and **c** RR195





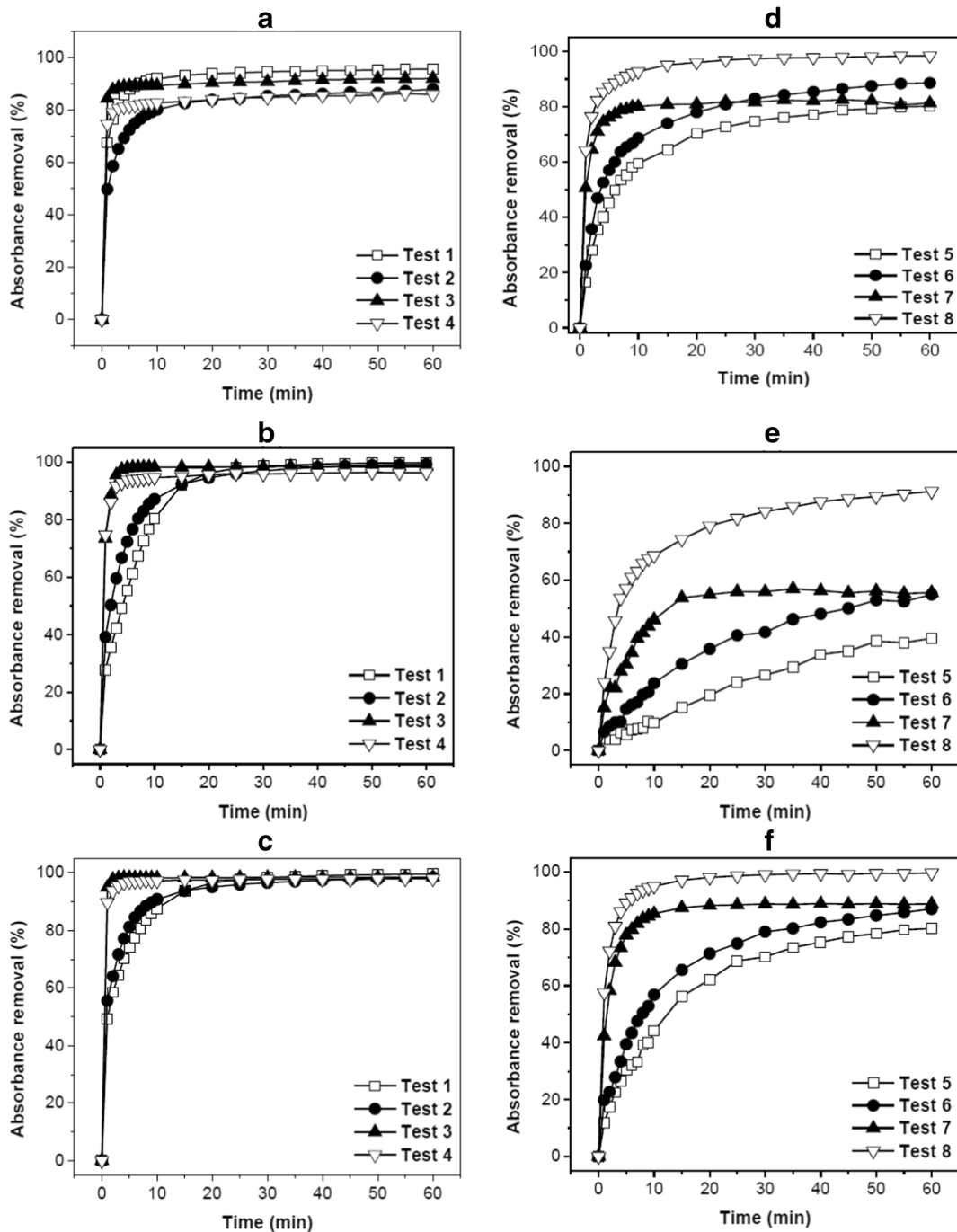


**Fig. 3** Reduction of the absorbance percentage at the specific wavelength of each dye. **a** RY145, **b** RB19, **c** RR195 (0.075 g L<sup>-1</sup>) and **d** RY145, **e** RB19, and **f** RR195 (0.75 g L<sup>-1</sup>)



where *S* represents all intermediate species formed and *k<sub>i</sub>* and *k<sub>j</sub>* are the overall velocity coefficients regarding reactions 13 and 14. The species are oxidized by <sup>•</sup>OH in

the reaction and will be represented by [*Oxi*]. Dye concentration regarding solution is absorbance (*Abs*). The corresponding kinetic equation to represent the reaction between dye and oxidizing species can be expressed by the following equations:

**Table 5** Kinetic constants of the effluent discoloration

Test	k (min <sup>-1</sup> )		
	RY145	RB19	RR195
1	1.0768	0.1459	0.1554
2	0.3438	0.1743	0.1777
3	–	–	–
4	–	–	–
5	0.1421	0.0087	0.0496
6	0.2082	0.0128	0.0708
7	0.3126	0.0509	0.1444
8	1.1678	0.0965	0.2298

- First-order kinetic model:

$$\frac{dAbs}{dt} = -k_i Abs [Oxi] \quad (15)$$

$$\frac{dAbs}{dt} = -k_{ap} Abs \quad (16)$$

- Second-order kinetic model:

$$\frac{dAbs}{dt} = -k_i Abs^2 [Oxi] \quad (17)$$

$$\frac{dAbs}{dt} = -k_{ap} Abs^2 \quad (18)$$

where

$$k_{ap} = \frac{k_i k_1 [H_2O_2] [Fe^{2+}]}{\sum k_j [S] [HO^*]} \quad (19)$$

Integrating eqs. 16 and 18, we have eqs. 20 and 21, corresponding to first- and second-order kinetics, respectively:

$$\ln\left(\frac{Abs_0}{Abs_t}\right) = k_{ap} t \quad (20)$$

$$\frac{1}{Abs} - \frac{1}{Abs_0} = k_{ap} t \quad (21)$$

Table 5 shows the kinetic velocity constants (k) obtained from the fit between models and experimental data. For the RY145 dye, the second-order model best fitted the experimental data. At lower concentrations of iron and peroxide, the kinetic constant for discoloration of the solution increases, when the concentration of pollutants is also the lowest. For higher concentrations of the pollutant, the decolorization kinetic constant increases when these Fenton reagents are in greater quantity.

For RB19 and RR195, the first-order kinetic model fitted better the experimental data. The constant increased with the same proportion of Fenton reactants. In the tests 3 and 4, the kinetic constants were not determined since the maximum reduction was obtained in the first 15 min of reaction.

### 3.3 Mixture of Dyes and Real Effluent

The optimized experimental conditions were used in order to treat a mixture solution of the three dyes aimed to verify the Fenton's potential for a complex effluent degradation. Figure 4a shows that the AR decreases significantly when the dye mix solution is treated. This behavior indicates a synergistically polluting effect between the dyes making degradation reaction less efficient. Besides, the possible formation of multiple by-products from dye oxidation and the interaction between the three compounds can reduce the removal efficiency as well (Rosales et al. 2009; Bouafia-Chergui et al. 2012). A real textile effluent was treated by Fenton using the optimized reaction conditions (Fig. 4b). In this case, absorbance removal percentage was lower than the mixture of dyes, obtaining just 22% after 1 h, which may be due to the complex mixture of the real effluent that contains much more contaminants that can quench the oxidant species.

### 3.4 Phytotoxicity Tests

In Fig. 5a, the germination index results, which are the effects of solutions on seeding growth and germination simultaneously, are shown using four dilutions (12.5, 25, 50, and 100%). Solutions treated in the optimal conditions did not present inhibitory effect on seed germination. GI values above 80% indicate no effects

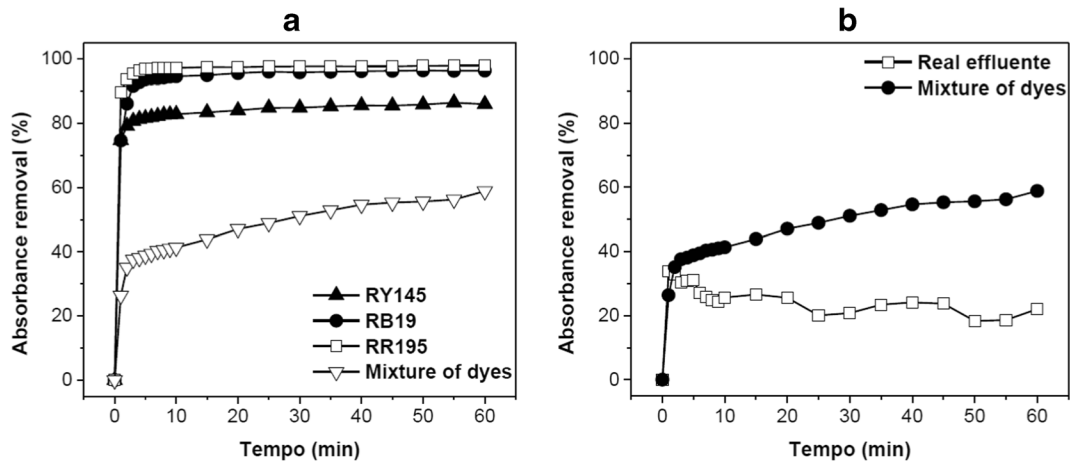


**Fig. 4** Decolorization comparison of the individual dyes and mixture of dyes (a) and the real effluent (b)

of phytotoxicity and values below 80% can be related to the inhibition of seed growth (Young et al. 2012; Xia et al. 2018). Thus, effluents that did not have toxic effects are those with values above 80% (indicated by the horizontal line). RB19 and RR195 were free of toxic effects after treatment. However, RY145 lost the toxicity only after 50% of dilution. The tests were performed for treated mixture of dyes solution and real textile effluent (Fig. 5b). The mixture of dye solution presented higher indexes when compared with real textile effluent; only below 25% of dilution, the toxic effects were eliminated. However, for the real textile effluent, the toxicity was eliminated only with 12.5% of dilution. These results may be due to the presence or formation of refractory compounds, or substances that react with Fenton reactants preventing the reaction. In addition, industrial effluent has greater complexity, containing other

substances than dyes, which can cause modifications in the oxygen demand, total dissolved solids, pH, turbidity, and other characteristics (Foo and Hameed 2010).

#### 4 Conclusions

The optimal Fenton reaction conditions for reactive dye removal were obtained using a 2<sup>3</sup> full factorial design of experiments coupled with a response surface methodology (RSM). The optimized conditions for higher values of absorbance reduction were 50 mg L<sup>-1</sup> of H<sub>2</sub>O<sub>2</sub> concentration, 0.5 mmol L<sup>-1</sup> of Fe<sup>2+</sup> concentration, and 0.075 g L<sup>-1</sup> of dye concentration. From kinetic studies, it is possible to observe second-order kinetic model fitted well the experimental data for RY145. First-

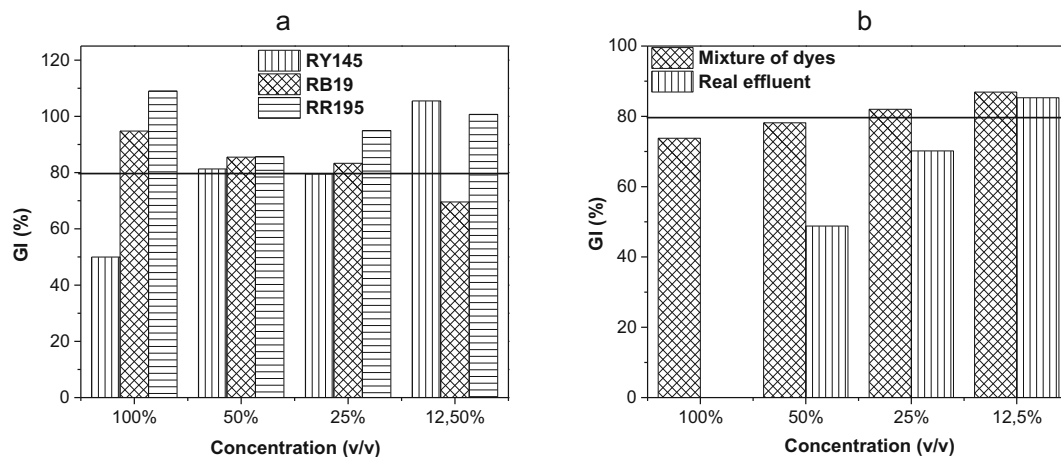


**Fig. 5** Seeds germination index in dyes (a) and effluents (b) after treatment

order kinetic model was the best one to represent experimental data for RB19 and RR195.

Evaluating the phytotoxicity tests, it was observed that the dye solutions treated in optimal Fenton conditions did not present inhibitory effects on seed germination. Phytotoxicity tests were performed for treated mixture of dye solution and real textile effluent, and Fig. 5 presents the germinate indexes. The mixture of dye solution presented higher germination indexes when compared with real textile effluent. For the first solution, below 25%, the toxic effects were eliminated, and for real wastewater, the toxicity was eliminated with 12.5%.

Considering the results obtained, Fenton reaction is quite efficient for effluent discoloration containing individual dyes. However, complex solutions, such as mixture of dyes and real effluents, a longer reactional time is necessary for efficient pollutant removal.

**Acknowledgments** The authors thank Conselho Nacional de Desenvolvimento Científico e Tecnológico (CNPq/Brazil), Coordenação de Aperfeiçoamento de Pessoal de Nível Superior (CAPES/Brazil), and Fundação de Amparo à Pesquisa do Estado de Alagoas (FAPEAL/Brazil).

## References

- Aksakal, O., & Uçun, H. (2010). Equilibrium, kinetic and thermodynamic studies of the biosorption of textile dye (Reactive Red 195) onto *Pinus sylvestris* L. *Journal of Hazardous Materials*, 181(1–3), 666–672. <https://doi.org/10.1016/j.jhazmat.2010.05.064>.
- Amiri, M. J., Bahrami, M., & Dehkhodaie, F. (2019). Optimization of Hg(II) adsorption on bio-apatite based materials using CCD-RSM design: characterization and mechanism studies. *Journal of Water and Health*, 17(4), 556–567. <https://doi.org/10.2166/wh.2019.039>.
- Asgher, M. (2012). Biosorption of reactive dyes: a review. *Water, Air, and Soil Pollution*, 223(5), 2417–2435. <https://doi.org/10.1007/s11270-011-1034-z>.
- Atkins, P., & Paula, J. D. (2009). Atkins' physical chemistry 8th edition. *Chemistry*. <https://doi.org/10.1021/ed056pA260.1>.
- Azha, S. F., Sellaoui, L., Engku Yunus, E. H., Yee, C. J., Bonilla-Petriciolet, A., Ben Lamine, A., & Ismail, S. (2019). Iron-modified composite adsorbent coating for azo dye removal and its regeneration by photo-Fenton process: synthesis, characterization and adsorption mechanism interpretation. *Chemical Engineering Journal*, 361, 31–40. <https://doi.org/10.1016/j.cej.2018.12.050>.
- Bahrpaima, K., & Fatehi, P. (2019). Preparation and coagulation performance of carboxypropylated and carboxypentylated lignosulfonates for dye removal. *Biomolecules*. <https://doi.org/10.3390/biom9080383>.
- Boczka, G., & Fernandes, A. (2017). Wastewater treatment by means of advanced oxidation processes at basic pH conditions: a review. *Chemical Engineering Journal*, 320, 608–633. <https://doi.org/10.1016/j.cej.2017.03.084>.
- Bouafia-Chergui, S., Oturan, N., Khalaf, H., & Oturan, M. A. (2012). A photo-Fenton treatment of a mixture of three cationic dyes. In *Procedia Engineering*. <https://doi.org/10.1016/j.proeng.2012.01.1192>.
- Bulut, Y., & Aydin, H. (2006). A kinetics and thermodynamics study of methylene blue adsorption on wheat shells. *Desalination*, 194(1–3), 259–267. <https://doi.org/10.1016/j.desal.2005.10.032>.
- Çiner, F. (2018). Application of Fenton reagent and adsorption as advanced treatment processes for removal of Maxilon Red GRL. *Global Nest Journal*. <https://doi.org/10.30955/gnj.002332>.
- da Silva Duarte, J. L., Meili, L., De Moura Gomes, L., Soletti, J. I., & de Zanta, C. L. (2019). Electrochemical process and Fenton reaction followed by lamellar settler to oil/surfactant effluent degradation. *Journal of Water Process Engineering*, 31, 100841. <https://doi.org/10.1016/j.jwpe.2019.100841>.
- de Lima, R. S., de Paiva e Silva Zanta, C. L., Meili, L., dos Santos Lins, P. V., de Souza dos Santos, G. E., & Tonholo, J. (2019). Fenton-based processes for the regeneration of biochar from *Syagrus coronata* biomass used as dye adsorbent. *Desalination and Water Treatment*. <https://doi.org/10.5004/dwt.2019.24343>.
- dos Santos, K. J. L., de Souza dos Santos, G. E., de Sá, Í. M. G. L., de Carvalho, S. H. V., Soletti, J. I., Meili, L., et al. (2019a). *Syagrus oleracea*-activated carbon prepared by vacuum pyrolysis for methylene blue adsorption. *Environmental Science and Pollution Research*, 26(16), 16470–16481. <https://doi.org/10.1007/s11356-019-05083-4>.
- dos Santos, K. J. L., de Souza dos Santos, G. E., de Sá, Í. M. G. L., Ide, A. H., da Silva Duarte, J. L., de Carvalho, S. H. V., et al. (2019b). *Wodyetia bifurcata* biochar for methylene blue removal from aqueous matrix. *Bioresource Technology*, 293, 122093. <https://doi.org/10.1016/j.biortech.2019.122093>.
- Dotto, J., Fagundes-Klen, M. R., Veit, M. T., Palácio, S. M., & Bergamasco, R. (2019). Performance of different coagulants in the coagulation/flocculation process of textile wastewater. *Journal of Cleaner Production*, 208, 656–665. <https://doi.org/10.1016/j.jclepro.2018.10.112>.
- Duarte, J. L. S., Soares, W. M. G., Gomes, L. M., Tonholo, J., & Zanta, C. L. P. S. (2013). Electrochemical oxidation of Safrrole using Ti/RuXTi(1 - X)O<sub>2</sub> system: preparation, characterization, and role of electrode composition. *Electrocatalysis*. <https://doi.org/10.1007/s12678-013-0153-2>.
- Duarte, J. L. S., Solano, A. M. S., Arguelho, M. L. P. M., Tonholo, J., Martínez-Huitle, C. A., & de Paiva e Silva Zanta, C. L. (2018). Evaluation of treatment of effluents contaminated with rifampicin by Fenton, electrochemical and associated processes. *Journal of Water Process Engineering*, 22, 250–257. <https://doi.org/10.1016/j.jwpe.2018.02.012>.
- Duarte, J. L. S., Meili, L., Gomes, L. M., Melo, J. M. O., Ferro, A. B., Tavares, M. G., et al. (2019). Electrochemical degradation of 17- $\alpha$ -methyltestosterone over DSA® electrodes. *Chemical Engineering and Processing - Process Intensification*, 142, 107548. <https://doi.org/10.1016/j.cep.2019.107548>.

- Elmoubarki, R., Mahjoubi, F. Z., Elhalil, A., Tounsadi, H., Abdennouri, M., Sadiq, M., et al. (2017). Ni/Fe and Mg/Fe layered double hydroxides and their calcined derivatives: preparation, characterization and application on textile dyes removal. *Journal of Materials Research and Technology*, 6(3), 271–283. <https://doi.org/10.1016/j.jmrt.2016.09.007>.
- Foo, K. Y., & Hameed, B. H. (2010). Decontamination of textile wastewater via TiO<sub>2</sub>/activated carbon composite materials. *Advances in Colloid and Interface Science*, 159(2), 130–143. <https://doi.org/10.1016/j.cis.2010.06.002>.
- Gagol, M., Przyjazny, A., & Boczkaj, G. (2018). Wastewater treatment by means of advanced oxidation processes based on cavitation—a review. *Chemical Engineering Journal*, 338, 599–627. <https://doi.org/10.1016/j.cej.2018.01.049>.
- Georgin, J., Franco, D. S. P., Grassi, P., Tonato, D., Piccilli, D. G. A., Meili, L., & Dotto, G. L. (2019). Potential of Cedrella fissilis bark as an adsorbent for the removal of red 97 dye from aqueous effluents. *Environmental Science and Pollution Research*, 26(19), 19207–19219. <https://doi.org/10.1007/s11356-019-05321-9>.
- Gonçalves, R. G. L., Lopes, P. A., Resende, J. A., Pinto, F. G., Tronto, J., Guerreiro, M. C., et al. (2019). Performance of magnetite/layered double hydroxide composite for dye removal via adsorption, Fenton and photo-Fenton processes. *Applied Clay Science*, 179, 105152. <https://doi.org/10.1016/j.clay.2019.105152>.
- Gui, L., Peng, J., Li, P., Peng, R., Yu, P., & Luo, Y. (2019). Electrochemical degradation of dye on TiO<sub>2</sub> nanotube array constructed anode. *Chemosphere*, 235, 1189–1196. <https://doi.org/10.1016/j.chemosphere.2019.06.170>.
- Guo, K., Gao, B., Tian, X., Yue, Q., Zhang, P., Shen, X., & Xu, X. (2019). Synthesis of polyaluminium chloride/papermaking sludge-based organic polymer composites for removal of disperse yellow and reactive blue by flocculation. *Chemosphere*, 231, 337–348. <https://doi.org/10.1016/j.chemosphere.2019.05.138>.
- Hassan, M. M., & Carr, C. M. (2018). A critical review on recent advancements of the removal of reactive dyes from dyehouse effluent by ion-exchange adsorbents. *Chemosphere*, 209, 201–219. <https://doi.org/10.1016/j.chemosphere.2018.06.043>.
- Hatimi, B., Nasrellah, H., Yassine, I., Joudi, M., El Mhammedi, M. A., Lançar, I. T., & Bakasse, M. (2018). Low cost MF ceramic support prepared from natural phosphate and titania: application for the filtration of disperse blue 79 azo dye solution. *Desalination and Water Treatment*. <https://doi.org/10.5004/dwt.2018.23238>.
- Kadam, A. A., Lade, H. S., Patil, S. M., & Govindwar, S. P. (2013). Low cost CaCl<sub>2</sub> pretreatment of sugarcane bagasse for enhancement of textile dyes adsorption and subsequent biodegradation of adsorbed dyes under solid state fermentation. *Bioresource Technology*, 132, 276–284. <https://doi.org/10.1016/j.biortech.2013.01.059>.
- Kalkan, N. A., Aksoy, S., Aksoy, E. A., & Hasirci, N. (2012). Adsorption of reactive yellow 145 onto chitosan coated magnetite nanoparticles. *Journal of Applied Polymer Science*, 124(1), 576–584. <https://doi.org/10.1002/app.34986>.
- Kaynar, Ü. H., Çınar, S., Çam Kaynar, S., Ayvaci, M., & Aydemir, T. (2018). Modelling and optimization of uranium (VI) ions adsorption onto nano-ZnO/chitosan bio-composite beads with response surface methodology (RSM). *Journal of Polymers and the Environment*, 26(6), 2300–2310. <https://doi.org/10.1007/s10924-017-1125-z>.
- Khatri, A., Peerzada, M. H., Mohsin, M., & White, M. (2015). A review on developments in dyeing cotton fabrics with reactive dyes for reducing effluent pollution. *Journal of Cleaner Production*, 87, 50–57. <https://doi.org/10.1016/j.jclepro.2014.09.017>.
- Li, X., Tang, S., Yuan, D., Tang, J., Zhang, C., Li, N., & Rao, Y. (2019). Improved degradation of anthraquinone dye by electrochemical activation of PDS. *Ecotoxicology and Environmental Safety*, 177, 77–85. <https://doi.org/10.1016/j.ecoenv.2019.04.015>.
- Liu, H., Qi, C., Feng, Z., Lei, L., & Deng, S. (2017). Adsorption of trace thorium(IV) from aqueous solution by mono-modified β-cyclodextrin polyrotaxane using response surface methodology (RSM). *Journal of Radioanalytical and Nuclear Chemistry*, 314(3), 1607–1618. <https://doi.org/10.1007/s10967-017-5518-1>.
- Liu, Y., Zhu, W., Guan, K., Peng, C., & Wu, J. (2018). Freeze-casting of alumina ultra-filtration membranes with good performance for anionic dye separation. *Ceramics International*, 44(10), 11901–11904. <https://doi.org/10.1016/j.ceramint.2018.03.160>.
- Luo, X., Liang, C., & Hu, Y. (2019). Comparison of different enhanced coagulation methods for azo dye removal from wastewater. *Sustainability (Switzerland)*. <https://doi.org/10.3390/su11174760>.
- Mahmoud, M. E., Nabil, G. M., El-Mallah, N. M., Bassiouny, H. I., Kumar, S., & Abdel-Fattah, T. M. (2016). Kinetics, isotherm, and thermodynamic studies of the adsorption of reactive red 195 A dye from water by modified Switchgrass Biochar adsorbent. *Journal of Industrial and Engineering Chemistry*, 37, 156–167. <https://doi.org/10.1016/j.jiec.2016.03.020>.
- Meili, L., Da Silva, T. S., Henrique, D. C., Soletti, J. I., De Carvalho, S. H. V., Da Silva Fonseca, E. J., et al. (2017). Ouricuri (*Syagrus coronata*) fiber: a novel biosorbent to remove methylene blue from aqueous solutions. *Water Science and Technology*, 75(1-2), 106–114. <https://doi.org/10.2166/wst.2016.495>.
- Meili, L., Lins, P. V., Zanta, C. L. P. S., Soletti, J. I., Ribeiro, L. M. O., Dormelas, C. B., et al. (2019a). MgAl-LDH/biochar composites for methylene blue removal by adsorption. *Applied Clay Science*, 168, 11–20. <https://doi.org/10.1016/j.clay.2018.10.012>.
- Meili, L., Godoy, R. P. S., Soletti, J. I., Carvalho, S. H. V., Ribeiro, L. M. O., Silva, M. G. C., et al. (2019b). Cassava (*Manihot esculenta* Crantz) stump biochar: physical/chemical characteristics and dye affinity. *Chemical Engineering Communications*. <https://doi.org/10.1080/00986445.2018.1530991>.
- Miklos, D. B., Remy, C., Jekel, M., Linden, K. G., Drewes, J. E., & Hübner, U. (2018). Evaluation of advanced oxidation processes for water and wastewater treatment—a critical review. *Water Research*, 139, 118–131. <https://doi.org/10.1016/j.watres.2018.03.042>.
- Mook, W. T., Ajeel, M. A., Aroua, M. K., & Szlachta, M. (2017). The application of iron mesh double layer as anode for the electrochemical treatment of Reactive Black 5 dye. *Journal*



- of *Environmental Sciences (China)*, 54, 184–195. <https://doi.org/10.1016/j.jes.2016.02.003>.
- Nascimento, R. C. S., Silva, A. O. S., & Meili, L. (2018). Carbon-covered mesoporous silica and its application in rhodamine B adsorption. *Environmental Technology (United Kingdom)*, 39(9), 1123–1132. <https://doi.org/10.1080/09593330.2017.1321693>.
- Nogueira, R. F. P., Trovó, A. G., da Silva, M. R. A., Villa, R. D., & de Oliveira, M. C. (2007). Fundamentos e aplicações ambientais dos processos fenton e foto-fenton. *Química Nova*. <https://doi.org/10.1590/s0100-40422007000200030>.
- Panizza, M., & Oturan, M. A. (2011). Degradation of Alizarin Red by electro-Fenton process using a graphite-felt cathode. *Electrochimica Acta*, 56(20), 7084–7087. <https://doi.org/10.1016/j.electacta.2011.05.105>.
- Priya, Sharma, A. K., Kaith, B. S., Tanwar, V., Bhatia, J. K., Sharma, N., et al. (2019). RSM-CCD optimized sodium alginate/gelatin based ZnS-nanocomposite hydrogel for the effective removal of bielrich scarlet and crystal violet dyes. *International Journal of Biological Macromolecules*, 129, 214–226. <https://doi.org/10.1016/j.ijbiomac.2019.02.034>.
- Qiu, J., Wang, H., Du, Z., Cheng, X., Liu, Y., & Wang, H. (2018). Preparation of polyacrylamide via dispersion polymerization with gelatin as a stabilizer and its synergistic effect on organic dye flocculation. *Journal of Applied Polymer Science*. <https://doi.org/10.1002/app.46298>.
- Rosales, E., Anasie, D., Pazos, M., Lazar, I., & Sanromán, M. A. (2018). Kaolinite adsorption-regeneration system for dye-stuff treatment by Fenton based processes. *Science of the Total Environment*, 622–623, 556–562. <https://doi.org/10.1016/j.scitotenv.2017.11.301>.
- Rosales, E., Pazos, M., Longo, M. A., & Sanromán, M. A. (2009). Electro-Fenton decoloration of dyes in a continuous reactor: a promising technology in colored wastewater treatment. *Chemical Engineering Journal*, 155(1–2), 62–67. <https://doi.org/10.1016/j.cej.2009.06.028>.
- Sathishkumar, K., AlSalhi, M. S., Sanganyado, E., Devanesan, S., Arulprakash, A., & Rajasekar, A. (2019). Sequential electrochemical oxidation and bio-treatment of the azo dye congo red and textile effluent. *Journal of Photochemistry and Photobiology B: Biology*. <https://doi.org/10.1016/j.jphotobiol.2019.11.1655>.
- Shamsuddin, N. M., Yusup, S., Ibrahim, W. A., Bokhari, A., & Chuah, L. F. (2015). Oil extraction from *Calophyllum inophyllum* L. via Soxhlet extraction: optimization using response surface methodology (RSM). In 2015 10th Asian Control Conference: Emerging Control Techniques for a Sustainable World, *ASCC 2015*. <https://doi.org/10.1109/ASCC.2015.7244791>.
- Shuang, S., Xing, X., Lejin, X., Zhiqiao, H., Haiping, Y., Jianmeng, C., & Bing, Y. (2008). Mineralization of CI reactive yellow 145 in aqueous solution by ultraviolet-enhanced ozonation. *Industrial and Engineering Chemistry Research*. <https://doi.org/10.1021/ie0711628>.
- Sohrabi, M. R., Khavaran, A., Shariati, S., & Shariati, S. (2017). Removal of Carmoisine edible dye by Fenton and photo Fenton processes using Taguchi orthogonal array design. *Arabian Journal of Chemistry*, 10(2), S3523–S3531. <https://doi.org/10.1016/j.arabjc.2014.02.019>.
- Song, Y., Hu, Q., Sun, Y., Li, X., Wan, H., Zang, L., et al. (2019). The feasibility of UF-RO integrated membrane system combined with coagulation/flocculation for hairwork dyeing effluent reclamation. *Science of the Total Environment*, 691, 45–54. <https://doi.org/10.1016/j.scitotenv.2019.07.130>.
- Sun, J. H., Sun, S. P., Fan, M. H., Guo, H. Q., Qiao, L. P., & Sun, R. X. (2007). A kinetic study on the degradation of p-nitroaniline by Fenton oxidation process. *Journal of Hazardous Materials*, 148(1–2), 172–177. <https://doi.org/10.1016/j.jhazmat.2007.02.022>.
- Tavares, M. G., Da Silva Santos, D. H., Albuquerque Torres, S. J., Oliveira Pimentel, W. R., Tonholo, J., & De Paiva Silva E Zanta, C. L. (2016). Efficiency and toxicity: comparison between the Fenton and electrochemical processes. *Water Science and Technology*, 74(5), 1143–1154. <https://doi.org/10.2166/wst.2016.278>.
- Tchounwou, P. B., Wilson, B. A., Ishaque, A. B., & Schneider, J. (2001). Toxicity tests to assess pollutants removal during wastewater treatment and the quality of receiving waters in Argentina. *Environmental Toxicology*, 16(3), 217–224. <https://doi.org/10.1002/tox.1027>.
- Thiam, A., Sirés, I., & Brillas, E. (2015). Treatment of a mixture of food color additives (E122, E124 and E129) in different water matrices by UVA and solar photoelectro-Fenton. *Water Research*, 81, 178–187. <https://doi.org/10.1016/j.watres.2015.05.057>.
- Vasconcelos, V. M., Ponce-De-León, C., Nava, J. L., & Lanza, M. R. V. (2016). Electrochemical degradation of RB-5 dye by anodic oxidation, electro-Fenton and by combining anodic oxidation-electro-Fenton in a filter-press flow cell. *Journal of Electroanalytical Chemistry*, 765, 179–187. <https://doi.org/10.1016/j.jelechem.2015.07.040>.
- Wang, W., & Freemark, K. (1995). The use of plants for environmental monitoring and assessment. *Ecotoxicology and Environmental Safety*, 30(3), 289–301. <https://doi.org/10.1006/eesa.1995.1033>.
- Wang, Z., Nguyen Song Thuy Thuy, G., Srivastava, V., Ambat, I., & Sillanpää, M. (2019). Photocatalytic degradation of an artificial sweetener (Acesulfame-K) from synthetic wastewater under UV-LED controlled illumination. *Process Safety and Environmental Protection*, 123, 206–214. <https://doi.org/10.1016/j.psep.2019.01.018>.
- Weber, C. T., Foletto, E. L., & Meili, L. (2013). Removal of tannery dye from aqueous solution using papaya seed as an efficient natural biosorbent. *Water, Air, and Soil Pollution*, 224, 1427. <https://doi.org/10.1007/s11270-012-1427-7>.
- Xia, M., Ye, C., Pi, K., Liu, D., & Gerson, A. R. (2018). Cr(III) removal from simulated solution using hydrous magnesium oxide coated fly ash: optimization by response surface methodology (RSM). *Chinese Journal of Chemical Engineering*. <https://doi.org/10.1016/j.cjche.2017.11.008>.
- Young, B. J., Riera, N. I., Beily, M. E., Bres, P. A., Crespo, D. C., & Ronco, A. E. (2012). Toxicity of the effluent from an anaerobic bioreactor treating cereal residues on *Lactuca sativa*. *Ecotoxicology and Environmental Safety*, 76(2), 182–186. <https://doi.org/10.1016/j.ecoenv.2011.09.019>.
- Zafar, M. S., Ahmad, S. W., Zia-Ul-Haq, M., Mubeen, A., & Khan, W. A. (2018). Removal of residual carcinogenic dyes from industrial wastewater using flocculation technique. *Chemical Industry and Chemical Engineering Quarterly*. <https://doi.org/10.2298/CICEQ160429024Z>.
- Zhijiang, C., Ping, X., Cong, Z., Tingting, Z., Jie, G., & Kongyin, Z. (2018). Preparation and characterization of a bi-layered

nano-filtration membrane from a chitosan hydrogel and bacterial cellulose nanofiber for dye removal. *Cellulose*, 25(9), 5123–5137. <https://doi.org/10.1007/s10570-018-1914-0>.

Zhou, Y., Xu, T., Zhang, Y., Zhang, C., Lu, Z., Lu, F., & Zhao, H. (2019). Effect of tea polyphenols on Curdlan/chitosan blend-

ing film properties and its application to chilled meat preservation. *Coatings*. <https://doi.org/10.3390/coatings9040262>.

**Publisher's Note** Springer Nature remains neutral with regard to jurisdictional claims in published maps and institutional affiliations.